

THEORETICAL EVALUATION OF THE NANOCARRIER PROPERTIES OF HYPERBRANCHED OLIGO (ETHYLENEIMINE) CASCADE GENERATIONS 1-5

JAVAD SAFAEI-GHOMI^{1a}, MEHRAN GHIACI^b, ZAHRA SADEGHI^a

^aDepartment of Organic Chemistry, Faculty of Chemistry, University of Kashan, 51167 Kashan, I. R. IRAN

^bDepartment of Chemistry, Isfahan University of Technology, Isfahan 8415683111, I. R. IRAN

The structures of N-(2-aminoethyl)-N-decylethane-1,2-diamine (ADD) based five families of hyperbranched oligo(ethyleneimine) (OEI) cascade generations 1-5 (CG 1-5) were designed as possible nanocarriers for some metals. They were optimized using the Molecular Mechanics, MM+ method. The PM3 Semi-Empirical Molecular Orbital Theory was used to optimize the structures of ADD-based hyperbranched cascade generations 1-5 (CG 1-5) and then investigated through the use of high-level density functional theory (DFT) methods. The peripheral molecular wave functions of CG1–5 are reactive, and were found to be a degenerate set with the similar eigenvalues. The reactivities of the peripheral orbitals allow the synthesis of larger generations. The bond lengths, shapes, sizes, energy stability of the CG1–5 structures and the size of the 3D structures were obtained. Quantum mechanical calculations have been carried out to study the structural and the electronic properties of CG1–5 adduct and some of their metal complexes. The optimized geometries, some of the calculated energies, spatial distribution and positions of HOMO, LUMO and the electrostatic potential of the molecules studied are obtained.

(Received April 2, 2010; accepted May 13, 2010)

Keywords: Hyperbranched Oligo(ethyleneimine); Nanocarrier; MM+ method; PM3 Semi-Empirical; Functional Theory DFT level B3LYP

1. Introduction

It was not until 1978 when Flory's vision became a reality. Vögtle *et al.* first reported the synthesis of a dendrimer, and then to a "cascade" molecule, via an iterative synthetic methodology [1]. This event is considered to be the "birth of dendritic or 'cascade' chemistry"[2].

Dendrites are unique synthetic macromolecules with highly branched structure and cascade shape [3-5]. Because molecular size and generation of dendrites are increased stepwise via the repetition of a reaction sequence, their size and structure are highly controllable and their molecular weight distribution is generally very narrow [5-7]. In addition, their interior has been shown to be capable of encapsulating various molecules [8-10]. Therefore, application of dendrites to drug delivery systems has been of great interest, although their use in this field has remained largely unexplored [11].

Dendrites are multi-branched (macro-) molecules often with highly symmetric structure. They can act as hosts for guest molecules capable of binding via non-covalent interactions such as Van der Waals interaction or hydrogen bonding [12, 13]. Dendrites can be functionalized with various functional groups and hence allow design of several novel applications, such as directional excitation energy transfer at molecular level [14]. Presence of several chromophores in a single

¹Corresponding author: safaei@kashanu.ac.ir or javad1338@hotmail.com

In this study and in continuation of our work on modification of solid supports, such as bentonite we would like to design a new family of dendritic molecules with lipophilic parts which could make strong Van der Waals interaction with organobentonites. For example, putting a long aliphatic chain on the studied molecules make them susceptible for immobilization on the hydrophobic surfaces for future applications. In this regard, we extended our computational investigations on the structures of OEI-based dendrites by adding a long aliphatic chain (C₁₆) to the dendrites and used the Molecular Mechanics (MM+) method, and the PM3 Semi-Empirical Molecular Orbital Theory [17] in our calculations. The geometry optimizations were carried out at the density functional theory (DFT) level (B3LYP), included in the Jaguar 5.5 program [18], using 3-21G* as the basis set (the latter in case of some metals, in order to incorporate the relativistic effects when many electrons are present [19]). Determining the most stable structure, at its lowest energy, provides vital information about the size, shape, and spatial orientations of dendrites. The delocalized molecular orbitals (DLMOs) in these dendrites can also be examined, which give information about their electronic structures and reactivities. These properties are important, because they govern the size of molecules, which can be encapsulated into the internal cavities, as well as the ability of dendrites to go through different barriers in different media.

2. Theoretical methods

Because dendrites are macromolecules which increase the size upon addition of each generation, it is necessary to choose a theoretical method capable of geometric characterization of such large structures. Initially, the molecular mechanics method with the MM+ force field was used to perform the calculations. The geometry optimization was carried out using the Polak–Ribiere conjugate gradient, set to terminate at an RMS gradient of 0.01 kcal Å⁻¹ mol⁻¹. Secondly, the semi-empirical parameterization model 3 (PM3) molecular orbital method, developed by Stewart [20, 21], was used with the Gaussian98 program [22]. Semi-empirical optimizations were carried out under standard convergence criteria (max force = 4.5 × 10⁻⁴ hartreesbohr⁻¹; RMS force = 3.0 × 10⁻⁴ hartreesbohr⁻¹; max displacement = 1.8 × 10⁻³ Å; RMS displacement = 1.2 × 10⁻³ Å). PM3 was chosen because it is a robust, accurate, semi-empirical theory, which always parallels experiment and is consequently predictive [23–26]. It is a particularly advantageous method to obtain conformational and chemical information about dendrites and then these structures were optimized and energies calculated at the B3LYP/3-21G* level of theory, by the variation method used previously [27]. The molecules were initially drawn in the HyperChem visualizer program [28], and optimized using molecular mechanics with MM+ force field, followed by the Gaussian98 program [22] to optimize the PM3 and then B3LYP structures. Dendrimeric structures were generated with the Chem3D-ultra (version 7.0) package [29]. Successive conformations of each system were generated by the integration of Newton's laws of motions, resulting in trajectories that specify how the positions and velocities of the particles in the systems vary with time, under Beeman's algorithm [30]. The resulting set of conformers was "cooled" by molecular mechanics calculations (MM+ force field) [31]. The interaction energies between dendrites (hosts) and metals (guests) were calculated according to the variation method [32], as the difference between the energy of the host – guest complex and the sum of energies of their isolated parts ($\delta E = E_{\text{host-guest complex}} - (E_{\text{host}} + E_{\text{guest}})$).

An initial qualitative approximation was carried out by MM2, considering the whole systems. The conformations of the dendrites were found by varying all torsional axes to discover the minimum global energy conformation, which was 8–9 kcal more stable than any other conformer. This minimum was established both by using the program in the PM3 Gaussian package, and also established independently using the Tree Branch Method [33]. OEI -based

dendrites (Fig. 1 shows generations 1 and 5) have recently become available in large quantities, and their synthesis is based on a simple and highly versatile methodology using primary amine group on the substrate was able to initiate the ring-opening polymerization of aziridine, resulting in highly branched poly(ethyleneimine) [34]. Dendrite generations 1–5 were optimized in a similar fashion by the molecular mechanics MM+ in the Hyper-Chem visualizer program [28].

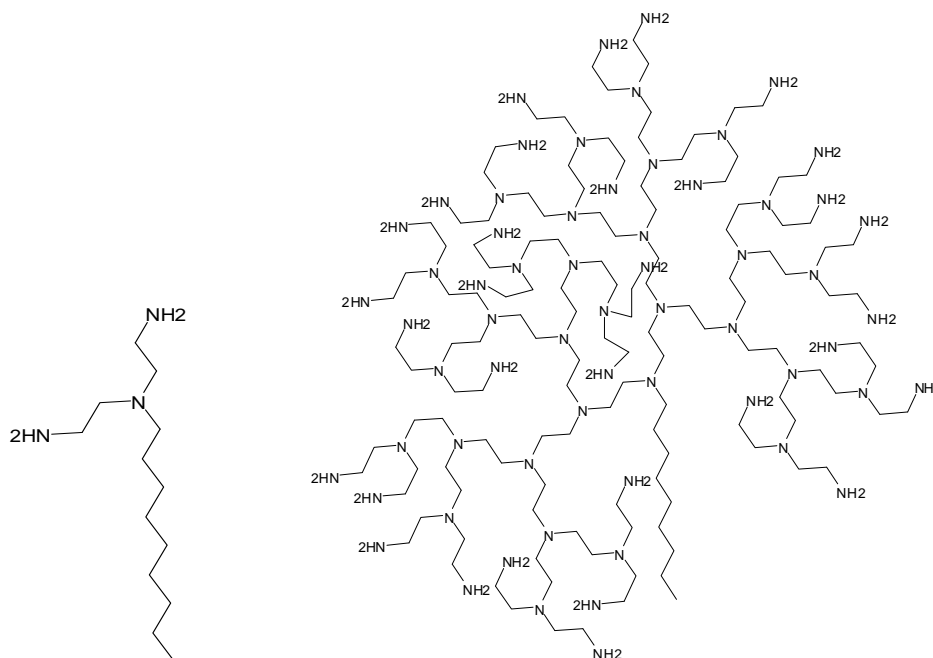


Fig.1. Hyperbranched cascade generations 1 and 5 (CG 1 and 5) of OEI-based dendrites

By comparison of the results, it was established that the MM+ molecular modeling results for CG1–3 were almost identical in conformation to the PM3 global minimum structures, and should consequently prove reliable and predictive for the CG4 and 5 conformations. Furthermore, PM3 single point calculations, using the Hyper-Chem visualizer program, on CG4 and 5 gave identical delocalized molecular orbitals (DLMO) on the periphery atoms to those found by PM3 in CG1–3. In order to compare PM3 energies from the same program, PM3 single point calculations and the geometry optimizations were carried out at the density functional theory (DFT) level (B3LYP), using the Gaussian98 program, were performed on CG4, but it was impossible to be completed for CG5 using ordinary computers, since it required a large memory. The energies are discussed later on in this paper. Fig. 2 shows the lowest unoccupied molecular orbitals (LUMO) for CG2 and 3, which are almost identical and to those in CG4–5 in terms of their locations on the periphery and their energies.

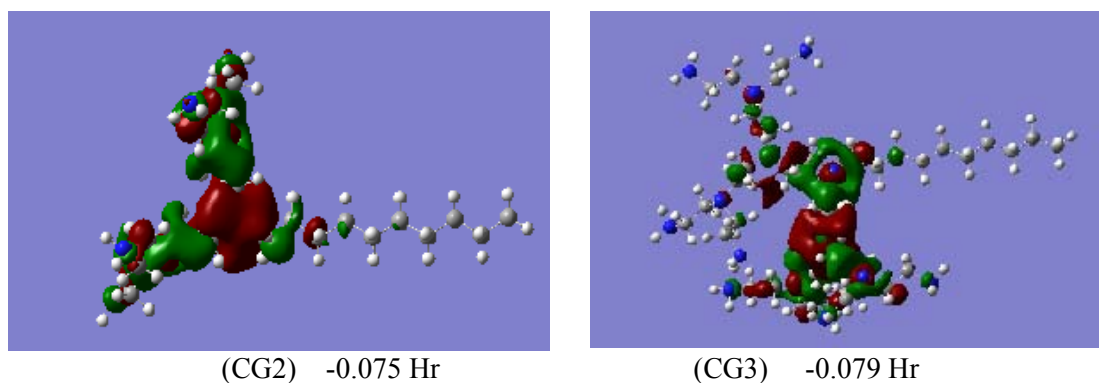


Fig.2. The lowest unoccupied molecular orbitals (LUMO) of CG2 and 3 and their energies.

Therefore, we can safely conclude that these DLMO do not change as the dendrite generation number increases, but they obviously multiply in number rapidly as the dendrite grows. This shows that OEI-based dendrites would behave in a similar manner, and the reactions that take place at all stages in forming the dendrites are identical. The DLMOs of CG4–5 are not shown because there are too many of them to be presented in this paper.

3. Results and discussion

3.1. Energies and terms of dendrimer generations 1-5

By using MM+, PM3 models and the B3LYP/DFT level of theory, by the 3-21G* method energies were calculated used previously (see under Computational Details). We have obtained the global energy conformations of CG1-5 (Table 1).

Table 1. Optimized conformational energies of CG1-5 using B3LYP/3-21G*/DFT, PM3 and MM+ methods

Hyperbranche generation no.	Energy (kcal/mol)		
	MM+	PM3	B3LYP/3-21G*
1	18.45	-61269.48	-717.69
2	44.41	-105221.52	-1246.61
3	94.51	-193127.19	-2312.45
4	180.86	-368926.23	-4444.19
5	299.17	-721407.36	-

B3LYP/3-21G* energies E(RB+HF-LYP) energy, PM3 energies are total energy, and MM+ are arbitrary energies in kcal/mol

The MM+ energies are conformational energies, and they are not related to heats of formation and nor to the total energies as computed by semi-empirical, PM3 and DFT methods. They do not have any physical meaning. However, these energies do include the effect of strained bond lengths, bond angles, torsional and non-bonded interactions. Probably in the lower generations the contribution of the bond length and bond angle strains in the total strain energy is not significant. By going to the higher generations the non-bonded interaction term becomes significant and one would expect that the bond length and bond angle strains contribute more in the total strain energy. Calculations show that the conformations from MM+, PM3 and DFT were identical for CG1-4. Therefore, it was assumed that the MM+ and PM3 conformation of CG5 can be used for single point calculations using the DFT method using the Gaussian98 program and the energy value for CG5 was obtained from the linear relationship between the PM3 and B3LYP/3-21G* energies and the dendrimer generation number for CG1-4 (PM3 method calculated for CG1-5) as shown in Fig. 3.

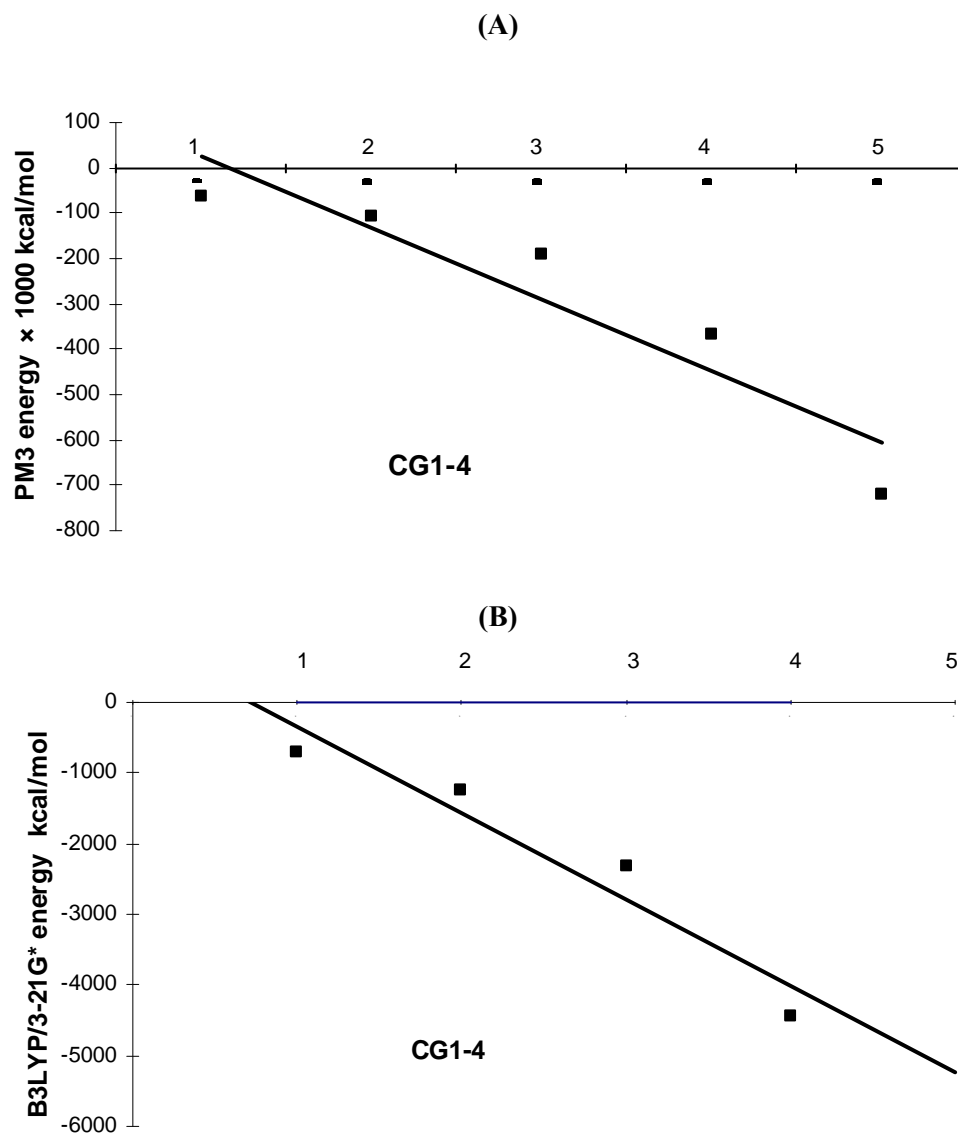
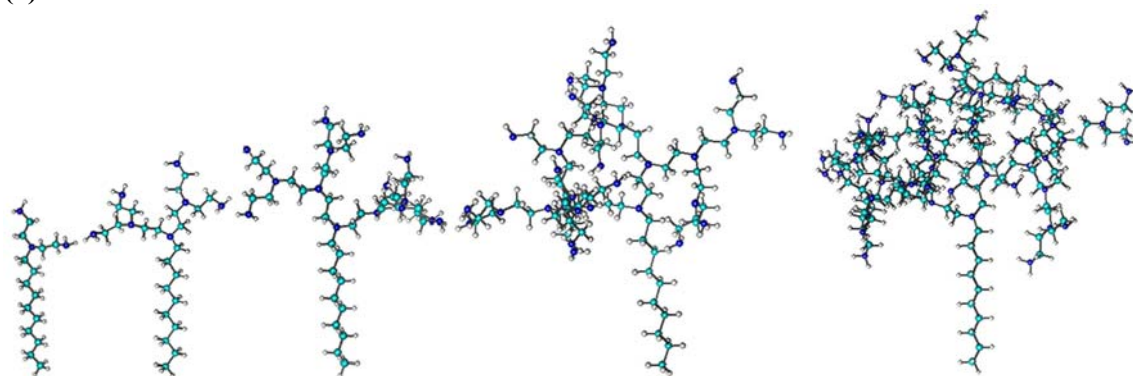


Fig. 3. The relationship between the dendrimer generation numbers and their corresponding (A) PM3 energies (B) B3LYP/3-21G* energies

3.2. Shapes of dendrimer generations 1-5

The shapes of dendrite generations 1-5 are shown in Fig. 4. The structures with the lowest energies were obtained by rotating several bonds in the dendrites to obtain a more symmetric structure with the least number of non-bonded interactions in MM+. Dendrimer generations 1-4 were then optimized using the DFT/B3LYP method to give identical structures as from the MM+ and PM3 method. The structures of dendrimer generations 4 and 5 were obtained from MM+ and PM3 calculations. It was assumed that these structures would be very close to those expected when optimized using the DFT method.

(a)



(b)

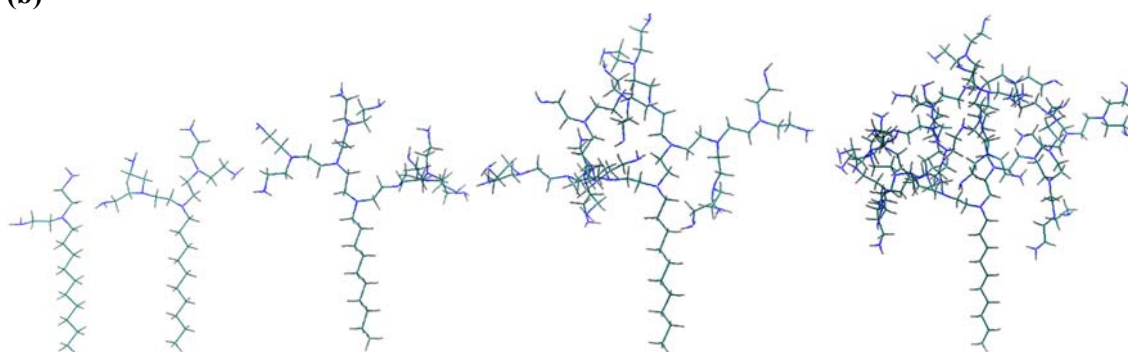


Fig.4. The optimized structures of hyperbranch cascade generations 1-5 using the molecular modeling MM+ method shown as (a) sticks and balls of side view of hyperbranch cascades (b) stick of side view of hyperbranch cascades to show clearly the development of the globular shape as the hyperbranch cascade generation increases.

Dendrite generation 1 (CG1) has a long aliphatic tail and two hydrophilic branches at the end of the molecule. In these hydrophilic branches the external amino groups are apart and do not show any internal hydrogen bonding. Table 2 shows the computed energies of the HOMO and LUMO molecular orbitals of the CG1-5 generations, calculated by PM3 and B3LYP/3-21G* methods. As one expects by going from one generation to the next one and as a result of packing of the branches, the gap between HOMO and LUMO should decrease. Because we have planned to use these dendrites for sensing drugs and trace elements, therefore in this step we tried to encapsulate different guest transition metal cations such as Zn^{2+} , Ni^{2+} , Fe^{2+} , Fe^{3+} , Cr^{3+} , Pd^{2+} and Cd^{2+} in the CG1-4.

Table 2. Computational E_{HOMO} and E_{LUMO} (eV) values for CG1-5 using PM3 and B3LYP/3-21G* methods.

Entry	PM3		B3LYP/3-21G*	
	HOMO	LUMO	HOMO	LUMO
CG1	-9.144	2.201	-0.20984	0.06780
CG2	-9.072	1.967	-0.15871	0.09354
CG3	-9.043	1.936	-0.16369	0.08243
CG4	-8.918	1.966	-0.15727	0.07509
CG5	-8.639	1.772	-	-

Table 3 shows the computed total energy (kcal/mol) values for CG1-4 for metal complexes using PM3 model. Probably, the difference between the energy of the host-guest complex and the sum of energies of their isolated parts are more informative, (Table 4). Our calculations show that there is an attractive interaction between the CG1-4 and Ni²⁺, Fe²⁺, Fe³⁺, Pd²⁺, Cr³⁺ cations. However, such an attractive interaction does not exist between the Zn²⁺ and Cd²⁺ cations and CG1-4. These data might be consistent because Zn²⁺ and Cd²⁺ have a close shell (d¹⁰) and probably do not have a low lying orbital for interaction with HOMO of the dendrites. Perhaps in the case of Pd²⁺, the size of the cation (0.86 Å) could play a role in these interactions, because it has the lowest tendency for such interactions.

Table 3. Computed total energy (kcal/mol) values for CG1-5 for metal complexes using PM3 model

Entry	Zn2+	Ni2+	Fe2+	Fe3+	Cr2+	Pd2+	Cd2+
No carrier	-631.576	-23810.068	-11901.457	-11901.457	-5467.202	-23810.068	-517.724
CG1	-61901.003	-85259.927	-73593.272	-73539.745	-66931.122	-85210.527	-61787.179
CG2	- 105853.650	- 129250.496	- 117618.194	- 117578.345	- 110978.651	- 129187.332	- 105740.001
CG3	- 193758.122	- 217196.994	- 205584.522	- 205506.963	- 198957.214	- 217126.255	- 193644.566
CG4	- 369516.308	- 393256.696	- 381765.624	- 381464.456	- 374841.454	- 392955.467	- 369411.356

Table 4. Computed difference between the energy of the host – guest complex ($\delta E = E_{\text{host-guest complex}} - (E_{\text{host}} + E_{\text{guest}})$).

Entry	Zn2+	Ni2+	Fe2+	Fe3+	Cr2+	Pd2+	Cd2+
CG1	0.056	-180.374	-422.330	-368.803	-194.435	-130.975	0.029
CG2	0.257	-218.096	-494.405	-454.556	-289.117	-154.933	0.054
CG3	0.652	-259.727	-555.866	-478.307	-362.813	-188.988	0.356
CG4	41.500	-520.395	-937.934	-636.766	-448.019	-219.166	32.600

HOMO and LUMO of the expected complexes between these molecules and different cations were also calculated, (Table 5). The energies of HOMO molecular orbitals of CG1-3 did not change in the case of their interactions with Zn²⁺, which is consistent with the data presented in the previous tables. Decrease in energy of the HOMO in the case of CG4 may not be surprising, because as the size of the dendrimer increases, the cation might find a reasonable interaction with the host. Decrease in energy of the HOMO molecular orbital of the CG1 when it interacts with Cd²⁺ is not clear to us.

Table 5. Computed E_{HOMO} and E_{LUMO} (eV) values for CG1-4 for metal complexes using PM3 model

Entry	Zn^{2+}		Ni^{2+}		Fe^{2+}		Fe^{3+}		Cr^{2+}		Pd^{2+}		Cd^{2+}	
	HOMO	LUMO	HOMO	LUMO	HOMO	LUMO	HOMO	LUMO	HOMO	LUMO	HOMO	LUMO	HOMO	LUMO
No carrier	-8.855	3.824	-17.84	0.032	-13.028	-0.194	-13.09	0.890	-6.238	2.504	-18.626	5.087	-6.621	23.556
CG1	-8.910	2.200	-7.662	1.820	-7.290	1.604	-7.973	2.330	-8.878	0.742	-8.767	2.254	-5.693	2.202
CG2	-8.876	2.166	-8.054	1.553	-8.103	0.762	-8.366	1.428	-8.961	-0.154	-8.802	2.156	-6.607	1.967
CG3	-8.849	1.925	-9.118	1.471	-8.408	0.364	-8.409	1.364	-9.492	-0.503	-8.856	1.991	-6.648	1.934
CG4	-6.415	1.824	-10.35	1.286	-8.834	0.012	-8.543	1.198	-10.52	-1.216	-9.167	1.254	-7.486	1.851

In the structure of CG2 the hydrophilic branches are still apart and probably do not give any recognizable internal cavity. Dendrimer generation 3 (CG3) shows a more spherical shape at the head of the molecule. The optimized structures of CG4 and CG5 both have a three dimensional globular heads, with well-defined internal cavities. The change in the 3D structure between CG1 and CG5 shows a clear progress in forming internal cavities in these dendrites, with increasing rigidity and more globular structure.

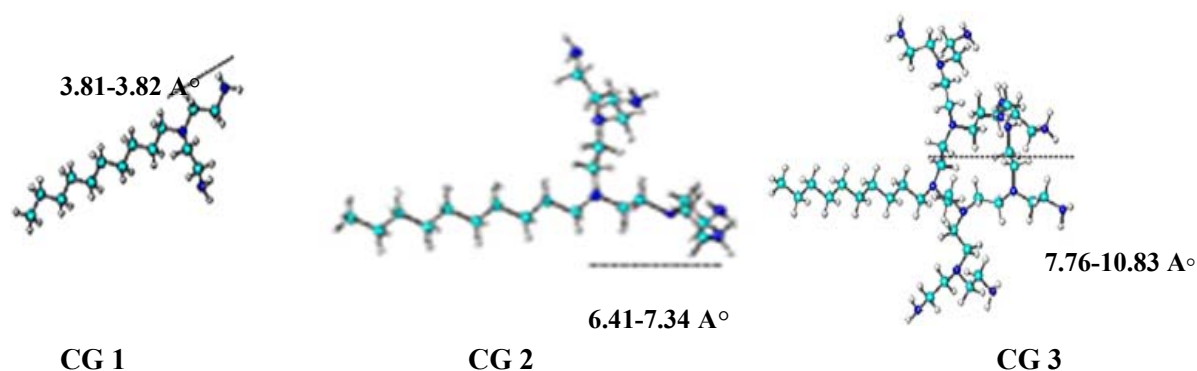


Fig. 5. CG1, CG2 and CG3 structures with their relative sizes (hyperbranched cascades)

It is predictable that a change in dendritic shape and crowding of the olig-ethyleneimine parts of the molecules should occur upon increasing the generation number. The relative diameters of the dendritic parts of the CG1-5 were obtained by measuring the distance between several pairs of peripheral atoms on opposite sides of the dendrimers as shown in Fig. 5 for CG1-4. A summary of the relative diameters of the globular heads of CG1-5 calculated using MM+, PM3 and DFT (B3LYP/3-21G*), and those of CG4-5 obtained using MM+ and PM3 are shown in Table 6. At the end, we would like to expose our fantasy by asking this question that “is it possible to have an aggregate of eight dendrimers that forms a micelle which the aliphatic tails has attractive interaction with each other on the core of the sphere?”, Fig. 6.

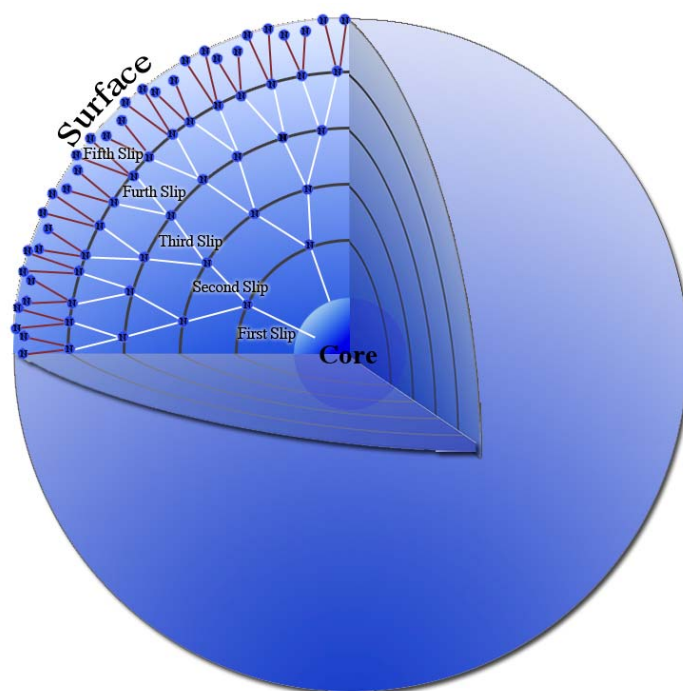


Fig. 6. A schematic representation of the space that occupied by generations CG (1-5)

4. Conclusions

Theoretical calculations using the molecular mechanics (MM+) method and the semi-empirical (PM3) molecular orbital theory and DFT (B3LYP/3-21G*) level has been shown very useful to obtain important information about lauryl amine based dendrimers.

Acknowledgements

Thanks are due to the Research Council of Isfahan University of Technology and Center of Excellency in the Chemistry Department of Isfahan University of Technology for supporting of this work.

References

- [1] E. Buhleier, W. Wehner, F. Vögtle, *Synthesis* 155 (1978).
- [2] G. R. Newkome, C. N. Moorefield, *Comprehensive Supramolecular Chemistry*; Reinholdt, D., Ed.; Pergamon: Oxford, UK, (1997).
- [3] D. A. Tomalia, A. M. Naylor, W. A. Goddard, *Angew. Chem., Int. Ed. Engl.* **29**, 138 (1990).
- [4] G. R. Newkome, C. N. Moorefield, F. Vögtle, *Dendritic molecules: concepts, syntheses, perspectives*, VCH, Weinheim (1996).
- [5] J. M. J. Fréchet, *Science* **263**, 1710 (1994).
- [6] D. A. Tomalia, H. Baker, M. Dewald Hall, G. Kallos, S. Martin, J. Roeck, J. Ryder, P. Smith, *Polym. J.* **17**, 117 (1985).
- [7] C. J. Hawker, J. M. J. Fréchet, *J. Am. Chem. Soc.* **4**, 8405 (1992).
- [8] J. F. G. A. Jansen, E. M. M. de Brabander-van den Berg, E. W. Meijer, *Science* **266**, 1226 (1994).
- [9] G. R. Newkome, C. N. Moorefield, G. R. Baker, M. J. Saunders, S. H. Grossman, *Angew. Chem., Int. Ed. Engl.* **30**, 1178 (1991).

- [10] G. Pistolis, A. Malliaris, D. Tsiourvas, C. M. Paleos, *Chem. Eur. J.* **5**, 1440 (1999).
- [11] M. Liu, J. M. J. Fréchet, *Pharm. Sci. Technol. Today* **2**, 393 (1999).
- [12] C.A. Schalley, F. Vögtle (Eds.), *Dendrimers IV*, *Top. Curr. Chem.* Vol. **17**, (2001).
- [13] A.W. Bosman, H.M. Janssen, E.W. Meijer, *Chem. Rev.* **99**, 1665 (1999).
- [14] F. Zeng, S.C. Zimmerman, *Chemical Reviews* **97**, 1681 (1997).
- [15] A. Adronov, J.M.J. Fréchet, *Chemical Commun.* 1701 (2000).
- [16] V. Balzani, P. Ceroni, S. Gestermann, M. Gorka, C. Kauffmann, F. Vögtle, *Tetrahedron* **58**, 629 (2002).
- [17] G.A. Segal, *Semiempirical Methods of Electronic Structure Calculation, Part A: Techniques*, University of Southern California, Los Angeles, (1997).
- [18] Jaguar5.0; Schrödinger; LLC: Portland, OR, (2000).
- [19] P. J. Hay, W. R. Wadt, *J Chem Phys* **82**, 299 (1985).
- [20] J.J.P. Stewart, *J. Comp. Chem.* **10** (2) 209 (1989).
- [21] J.J.P. Stewart, *J. Comp. Chem.* **10** (2) 221 (1989).
- [22] Gaussian 98W (Revision A.5), M.J. Frisch, G.W. Trucks, H.B. Schlegel, G.E. Scuseria, M.A. Robb, J.R. Cheeseman, V.G. Zakrzewski, J.A. Montgomery, R.E. Stratmann, J.C. Burant, S. Dapprich, J.M. Millam, A.D. Daniels, K.N. Kudin, M.C. Strain, O. Farkas, J. Tomasi, V. Barone, M. Cossi, R. Cammi, B. Mennucci, C. Pomelli, C. Adamo, S. Clifford, J. Ochterski, G.A. Petersson, P.Y. Ayala, Q. Cui, K. Morokuma, D.K. Malick, A.D. Rabuck, K. Raghavachari, J.B. Foresman, J. Cioslowski, J.V. Ortiz, B.B. Stefanov, G. Liu, A. Liashenko, P. Piskorz, I. Komaromi, R. Gomperts, R.L. Martin, D.J. Fox, T. Keith, M.A. Al-Laham, C.Y. Peng, A. Nanayakkara, C. Gonzalez, M. Challacombe, P.M.W. Gill, B.G. Johnson, W. Chen, M.W. Wong, J.L. Andres, M. Head-Gordon, E.S. Replogle, J.A. Pople, Gaussian, Inc., Pittsburgh, PA, (1998).
- [23] A. Dickie, A.K. Kakkar, M.A. Whitehead, *Langmuir* **18**, 5657 (2002).
- [24] F. Rakotonradany, M.A. Whitehead, A. Lebuis, H.F. Sleiman, *Chem. Eur. J.* **9**, 4771 (2003).
- [25] P. Charbonneau, B. Jean-Claude, M.A. Whitehead, *J. Mol. Struct. (Theochem.)* **574**, 85 (2001).
- [26] C. Malardier-Jugroot, A.C. Spivey, M.A. Whitehead, *J. Mol. Struct. (Theochem.)* **623**, 263 (2003).
- [27] A. Evangelista-Lara, P. Guadarrama, *International Journal of Quantum Chemistry*, **103**, 460 (2005).
- [28] HyperChem release 5.11. For Windows molecular modeling system, Hypercube Inc., 419 Philip Street, Waterloo, Ont., Canada N2L 3X2, (1999).
- [29] Chem3D Ultra version 7.0 (2002); CambridgeSoft Corporation, (1986–2002).
- [30] D. Beeman, *J Comput Phys*, **20**, 130 (1976).
- [31] U. Burkert, N. L. Allinger, *Molecular Mechanics*; ACS Monograph No. 177; American Chemical Society: Washington, DC, (1982).
- [32] K. Muller-Dethlefs, P. Hobza, *Chem Rev*, **100**, 143 (2000).
- [33] F. Villamagna, M.A. Whitehead, *J. Chem. Soc., Faraday Trans.* **90**, (1) 47 (1994).
- [34] C.O. Kim, S. J. Cho, J.W. Park *Journal of Colloid and Interface Science* **260**, 374 (2003).